SUPPLEMENTARY INFORMATION

Use of Organic Bulk-heterojunction Solar Cells as Selective Contacts in Wide Band-Gap Perovskite Solar Cells: Advantages and Limitations.

Lijun Su,[a,b] Maria Méndez Màlaga,[b] Miaoli Zhu,[a]* Yaoming Xiao,[c]* and Emilio Palomares Gil[b,d]*

[a] *Institute of Molecular Science, Key Laboratory of Chemical Biology and Molecular Engineering of Education Ministry, Innovation Center of Chemistry and Molecular Science, Key Laboratory of Materials for Energy Conversion and Storage of Shanxi Province, Shanxi University, Taiyuan, 030006, PR China*
[b] *Institute of Chemical Research of Catalonia (ICIQ), The Barcelona Institute of Science and Technology (BIST), Avda. Països Catalans, 16, Tarragona, E-43007, Spain*
[c] *College of Chemical Engineering and Materials Science, Quanzhou Normal University, Quanzhou, 362000, PR China*
[d] *ICREA, Passeig Lluís Companys, 23, Barcelona, E-08010, Spain*

**corresponding authors: miaoli@sxu.edu.cn, ymxiao@qztc.edu.cn, epalomares@iciq.es*

Experimental Method

Fabrication of devices

Fluorine tin oxide (FTO)-coated glass substrates were first brushed with water and Hellmanex™ soap, then, they were ultrasonicated with distilled water, acetone, and isopropanol sequentially. Finally, they were dried with an air flow and treated with UV ozone for 30 minutes.

A compact TiO_2 layer was deposited onto the substrates by spin-coating 0.3 M $Ti(iPrO)_2(acac)_2$ solution in 2-propanol using 4000 rpm, 1000 rpm/s for 25 s, then followed by thermal annealing at 125 °C for 5 minutes and 450 °C for 30 minutes. Once the substrates cooled down, they were immersed into a 40 mM $TiCl_4$ solution at 70 °C for 30 minutes. After that, they were cleaned with distilled water and ethanol and dried with a strong air flow.

To deposit the mesoporous TiO_2 layer, a solution with a 30 nm particle size was prepared by diluting a commercial paste (30NR-D, Greatcell) in ethanol (1:7 weight ratio) with 6000 rpm, 1000 rpm/s for 30 s. Then, they were annealed using same conditions for compact TiO_2 layer.

Perovskite layer deposition

For perovskite layer, 1 M solution of $MAPbBr_3$, $MAPbIBr_2$, and $MAPbI_2Br$ were made by using below formulas to dissolve MAI, MABr, PbI_2 or $PbBr_2$ into DMF:DMSO (4:1, volume ratio), respectively. Then, the solution was filtered and spin-coated onto the mesoporous titania film with a two-step program, first 2000 rpm, 1000 rpm/s for 12 s, and then 5000 rpm, 2000 rpm/s for 25 s. 10 seconds before the end of the spinning process, 100 µl of chlorobenzene were dropped in the center of the substrate while spinning. For $MAPbI_3$, two-step approach was used to gain a better perovskite surface morphology. First, 1 M PbI_2 solution dissolved in DMF:DMSO (9:1, volume ratio) was spin-coated at 2000 rpm, with 2000 rpm/s for 90 s. Then, 100 µl MAI (50 mg/ml in 2-propanol) was deposited on the last 30 seconds before the spinning process ended. Finally, all kinds of perovskite layers were annealed at 100 °C for 60 minutes. We prepared the devices into a glovebox and by using a continuous N_2 flow to remove the solvent atmosphere that may affect the perovskite morphology.

The following formulas indicate the salts involved for the fabrication of the different perovskite compositions:

$MAI + PbI_2 \longrightarrow MAPbI_3$

$MABr + PbI_2 \longrightarrow MAPbI_2Br$

$MAI + PbBr_2 \longrightarrow MAPbIBr_2$

$MABr + PbBr_2 \longrightarrow MAPbBr_3$

Organic layer depostion

In the case of perovskite/BHJ integrated solar cells, the materials (PM6:Y6=1:1.2, 16 mg/ml) were dissolved in chloroform with the solvent additive of 1-chloronaphthalene (0.5%, volume ratio) and spin-coated at 3000 rpm for 30 s onto the perovskite layer.

As a reference, 60 mM spiro-OMeTAD solution was prepared as hole transporting material. To this solution, we added 4-tert-butylpyridine, LiTFSI and Co(III) TFSI. 35 µl of this solution was spin-coated at 4000 rpm, 2000 rpm/s for 30 s on perovskite layer.

Finally, for perovskite/spiro-OMeTAD devices, 80 nm Au was thermal evaporated under high vacuum conditions and for perovskite/BHJ integrated devices, 15 nm MoO_3 was thermal evaporated as a buffer layer before Au deposition. The MoO_3 can protect the organic film from damage caused by Au deposition as well as a layer to build the ohmic contact for hole extraction from BHJ to the Au electrode.

Characterization techniques

The crystalline structure of perovskite has been determined using X-Ray Diffraction (XRD). The measurements were made from samples deposited on FTO/TiO_2 mesoporous substrates and using a Siemens D5000 diffractometer (Bragg-Brentano parafocusing geometry and vertical θ-θ goniometer) fitted with a curved graphite diffracted-beam monochromator, incident and diffracted beam Soller slits, a 0.06º receiving slit and scintillation counter as a detector. The angular 2θ diffraction range was between 10 and 60º. The data were collected with an angular step of 0.05º at 3 s per step and sample rotation. CuK_α radiation was obtained from a copper X-ray tube operated at 40 kV and 30 mA.

Field Emission Scanning Electron Microscopy (FESEM) was used in FEI Quanta 600 microscopy to obtain the cross-section images in order to observe all the layers of a complete device.

The J-V curves were measured using a Solar Simulator (ABET 11000) and a source meter (Keithley 2400). The curves were registered under 1 Sun conditions (100 mW/cm^2, AM 1.5G) calibrated with a Si-reference cell. The active area of the devices was 0.09 cm^2. The scan rate employed was 0.08V/s. For the measurements with different light intensities, different optical filters were employed.

All the external quantum efficiency data were recorded by quantum efficiency measurement systems from Lasing, S.A. (IPCE-DC, LS1109-232), and a Newport 2936-R power-meter unit. The EQE measurements were taken under wavelength sweep from 300 nm to 1100 nm.

Ultraviolet and visible spectrum (UV-Vis) measurements were done in an Agilent Cary 60 UV-Vis Spectrophotometer with two silicon detectors, double beam optics, Czerny-Turner monochromator, 190-1100 nm range and the light source is a Xenon Flash Lamp.

Photo-induced charge extraction (CE) and transient photovoltage (TPV) measurements were carried out using a white LED controlled by a programmable power supply and a control box that switches from open to short-circuit states. All the signals are recorded in an oscilloscope Yokogawa DLM2052 registering drops in voltage. Light perturbations pulses for TPV and TPC were provided by a nanosecond PTI GL-3300 nitrogen laser and using a 525 nm laser pulse wavelength. **Scheme S1** shows the TPV set up.

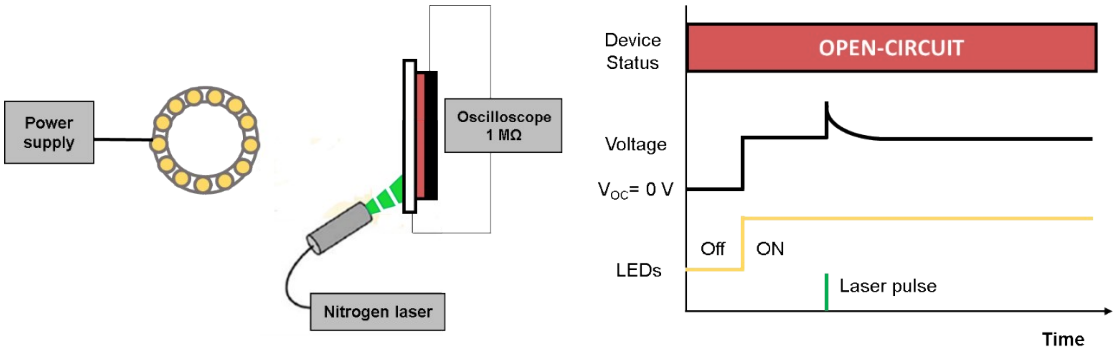

Scheme S1. Set up used to obtain transient photovoltage decays (left) and the corresponding processes occurring during the measurements (right).

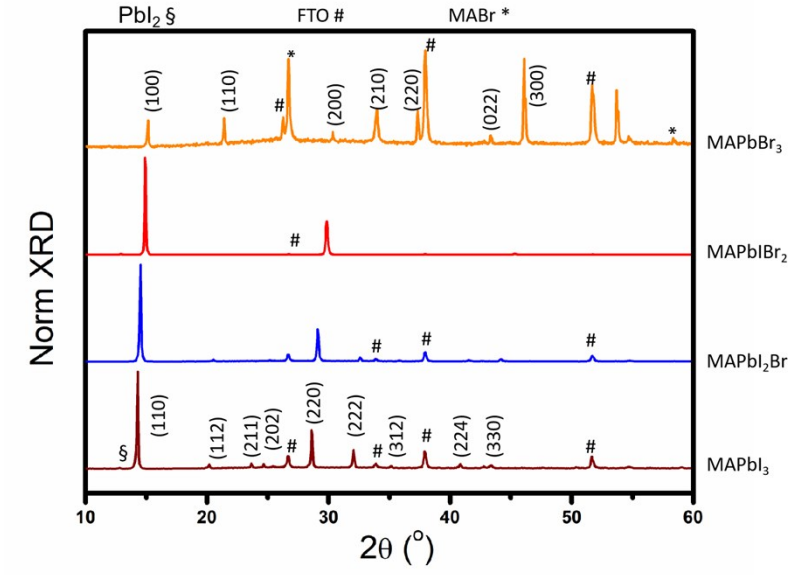

Figure S1. XRD patterns of the four different perovskite compositions used in this work with their corresponding peaks.

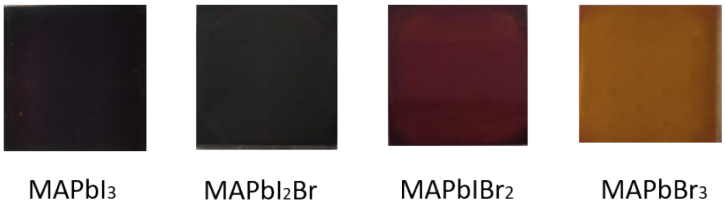

Figure S2. Photographs of the $MAPbI_{3-x}Br_x$ solar cells fabricated in this work.

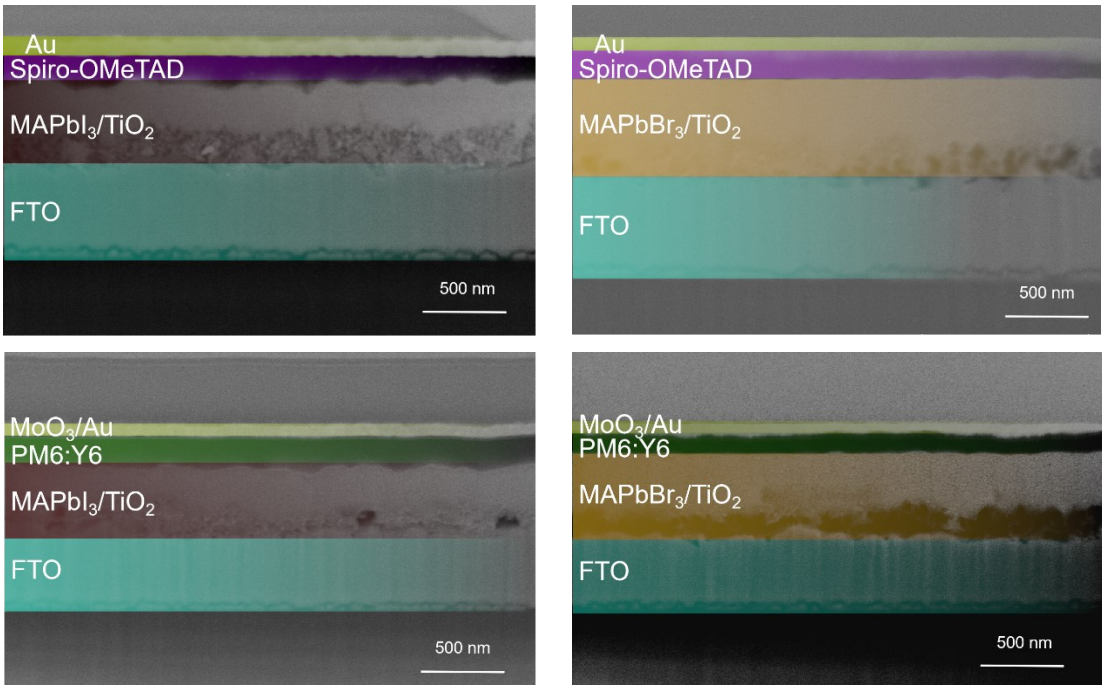

Figure S3. Cross section images of $MAPbI_3$ and $MAPbBr_3$ devices with spiro-OMeTAD and OPV layer.

Table S1. Photovoltaic performances of $MAPbI_{3-x}Br_x$/spiro-OMeTAD and $MAPbI_{3-x}Br_x$/(PM6:Y6) devices (resulting from the average values of 8 devices), under the illumination of AM 1.5 G, 100 Mw/cm^2.

Devices	**Sweep**	**Jsc (mA/cm^2)**	**Voc (V)**	**FF**	**PCE(%)**
$MAPbI_3$/spiro-OMeTAD	Forward	18.99±1.69	1.01±0.04	0.63±0.01	14.16±1.28
	Reverse	19.65±1.45	1.00±0.01	0.70±0.05	15.43±1.18
$MAPbI_3$/(PM6:Y6)	Forward	22.48±1.32	0.93±0.03	0.40±0.04	9.36±1.25
	Reverse	14.15±1.26	0.90±0.05	0.44±0.03	10.25±0.96
$MAPbI_2Br$/spiro-OMeTAD	Forward	14.06±1.35	0.86±0.05	0.44±0.04	5.34±0.73
	Reverse	14.50±1.21	0.95±0.04	0.61±0.08	8.38±0.83
$MAPbI_2Br$/(PM6:Y6)	Forward	16.78±1.34	0.87±0.01	0.50±0.02	7.34±0.55
	Reverse	16.22±0.71	0.88±0.02	0.47±0.01	6.93±0.69

$MAPbIBr_2$/spiro-OMeTAD	Forward	7.56±1.5	1.10±0.06	0.49±0.07	3.92±0.73
	Reverse	4.50±0.69	0.96±0.05	0.63±0.09	2.72±0.82
$MAPbIBr_2$/(PM6:Y6)	Forward	12.64±1.28	1.07±0.04	0.36±0.03	5.67±0.69
	Reverse	11.98±0.97	1.01±0.05	0.40±0.04	5.08±0.74
$MAPbBr_3$/spiro-OMeTAD	Forward	5.49±0.96	1.29±0.11	0.62±0.01	5.47±0.67
	Reverse	5.61±1.12	1.34±0.09	0.68±0.03	6.46±0.55
$MAPbBr_3$/(PM6:Y6)	Forward	5.99±0.45	1.25±0.04	0.44±0.07	4.18±0.36
	Reverse	6.00±0.68	1.33±0.06	0.60±0.05	4.96±0.24

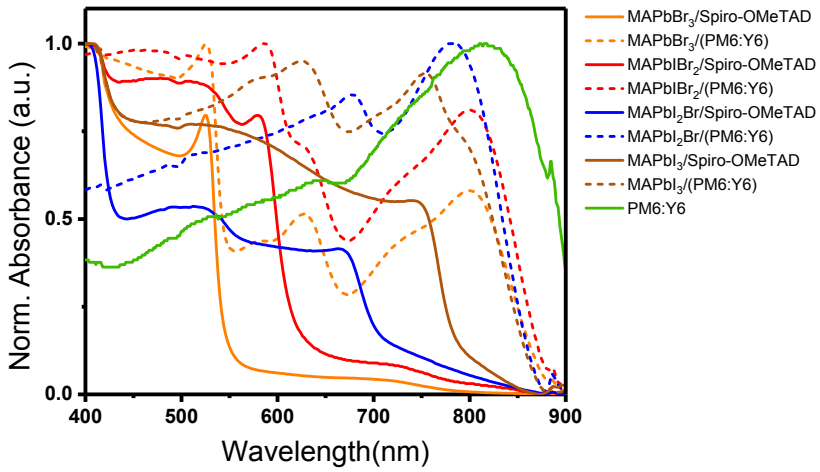

Figure S4. Absorption spectra of the different $MAPbI_{3-x}Br_x$/spiro-OMeTAD, $MAPbI_{3-x}Br_x$/OPV and OPV films.

Transient Photovoltage

$MAPbI_3$/spiro-OMeTAD

The mechanisms occurring in a TPV measurement of a complete cell made of $MAPbI_3$/spiro-OMeTAD are illustrated in **Fig. S5**. This diagram mainly describe the situation before cell reaches the equilibrium.[1,2] Very briefly, when the cell is under dark conditions, the ions presented in perovskite bulk material migrates to the respective contact interfaces creating a double layer.[3] At the initial illumination response **(a)**, an electric field opposing the normal direction of carrier transport will exist near their respective blocking contacts. This electric field creates an accumulation of electrons and holes and it remains until the ions have had time to discharge from the interfacial layers. When the cell is illuminated with an extra laser pulse **(b)**, the electric field becomes more unfavorable, increasing the carrier accumulation in the regions of high rates of recombination. This will increase the rate of recombination and will produce the negative transient signal when the laser is switched on. Once the increased charge accumulation shields

the potential valleys near the contacts, the photovoltage is able to recover and becomes positive **(c)**.

Since the TPV were recorded when the cell reaches the equilibrium, we did not observed the negative transient decays for the cells with spiro-OMeTAD as HTM.

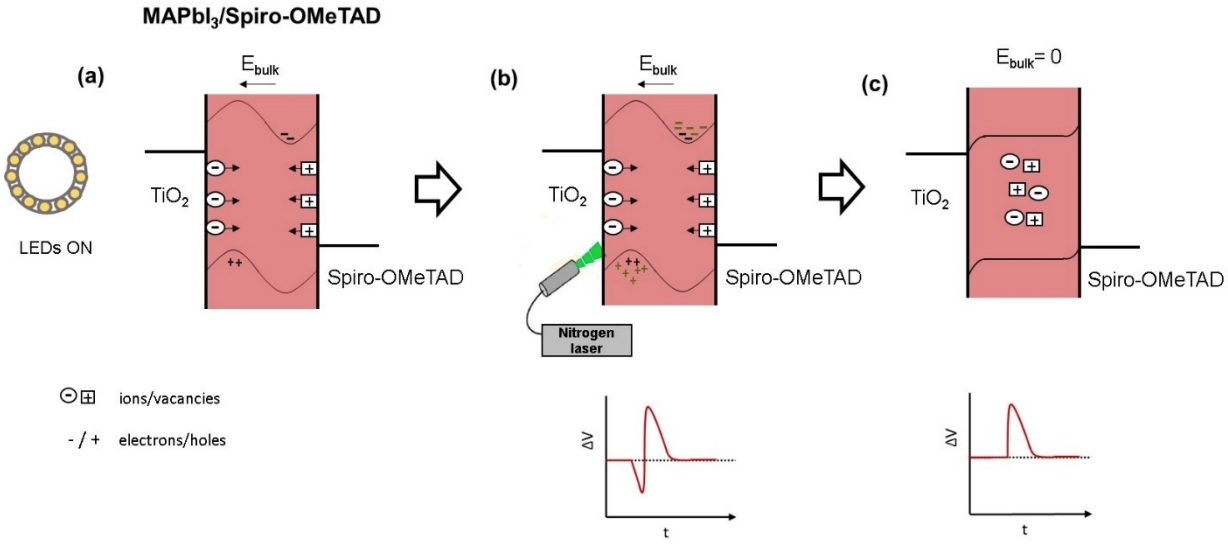

Fig. S5. Diagram of the mechanisms occurring in a cell of $MAPbI_3$/spiro-OMeTAD during a TPV measurement.

The case explained above is valid for all the cells with spiro-OMeTAD as HTM. However, some perovskite compositions with PM6:Y6 in their structures, show a "permanent" negative transient, especially at high illumination intensities (for instance TPV of $MAPbI_3$/OPV cell shown in **Fig. 11a**).

<u>$MAPbI_3$/OPV</u>

In order to understand the mechanisms in the $MAPbI_3$/PM6:Y6 interface during the TPV measurements, **Fig. S6** depicts an example of this case. We might suppose the same scenario occurring in the perovskite layer as shown above, an electric field exists and when the laser pulse switches off, the recombination mitigates and the voltage increase becoming positive **(a, b)**. However, the PM6:Y6 is acting as a functional solar cell, where the electrons and holes are being created and so, an extra charges should move to the corresponding contact. Those extra charges may not be allowed to the cell shield the potential valleys near the contacts **(c)**. Therefore, for the TPV measurements taken at low illumination intensities (approaching to dark), the charges accumulation decreases enough resulting in positive voltage recovery.

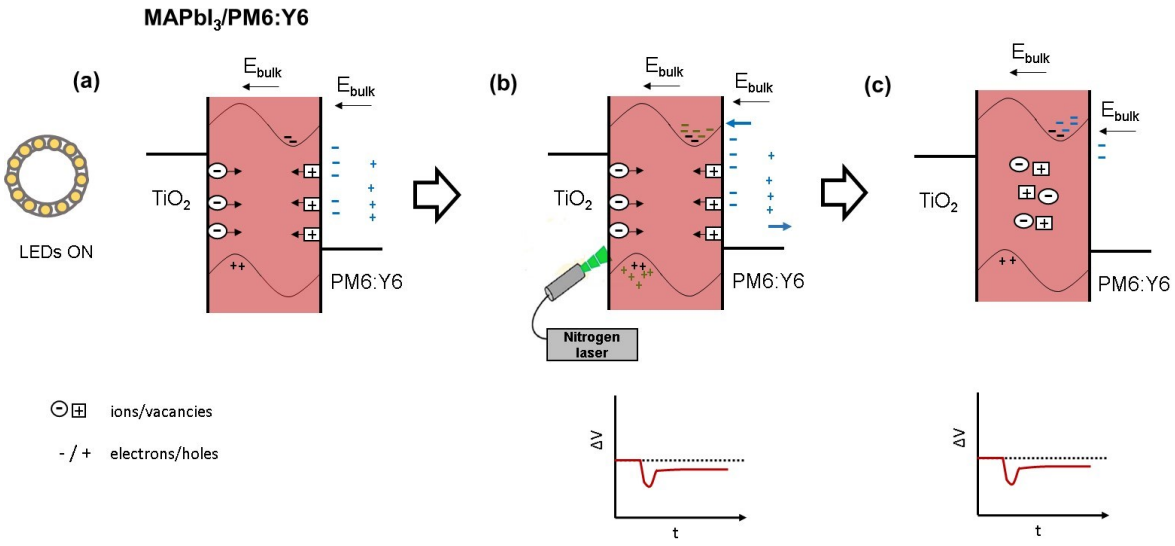

Fig. S6. Diagram of the mechanisms occurring in a cell of $MAPbI_3$/PM6:Y6 during a TPV measurement.

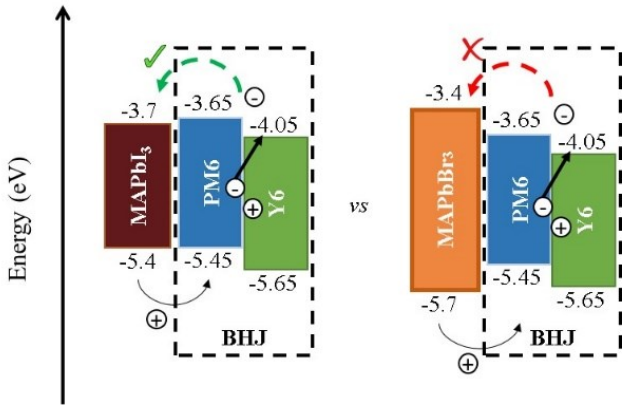

Fig. S7. Energy diagrams for $MAPbI_3$/PM6:Y6 and $MAPbBr_3$/PM6:Y6.

References

1 A. Pockett and M. J. Carnie, *ACS Energy Lett.*, 2017, **2**, 1683–1689.

2 P. Calado, D. Burkitt, J. Yao, J. Troughton, T. M. Watson, M. J. Carnie, A. M. Telford, B. C. O'Regan, J. Nelson and P. R. F. Barnes, *Phys. Rev. Appl.*, 2019, **11**, 44005.

3 A. Pockett, G. E. Eperon, N. Sakai, H. J. Snaith, L. M. Peter and P. J. Cameron, *Phys. Chem. Chem. Phys.*, 2017, **19**, 5959–5970.